Applied Physics Letters

Current switching of interface antiferromagnet in ferromagnet/antiferromagnet heterostructure

Cite as: Appl. Phys. Lett. **118**, 032402 (2021); https://doi.org/10.1063/5.0039074
Submitted: 30 November 2020 . Accepted: 29 December 2020 . Published Online: 19 January 2021

Z. Yan, J. J. Yun, W. B. Sui, L. Xi, Z. T. Xie, J. W. Cao, M. S. Si, D. Z. Yang, and D. S. Xue

COLLECTIONS

Note: This paper is part of the Special Topic on Spin-Orbit Torque (SOT): Materials, Physics and Devices.

This paper was selected as an Editor's Pick

AIP Publishing

Applied Physics Letters ARTICLE scitation.org/journal/apl

Current switching of interface antiferromagnet in ferromagnet/antiferromagnet heterostructure

Cite as: Appl. Phys. Lett. **118**, 032402 (2021); doi: 10.1063/5.0039074
Submitted: 30 November 2020 · Accepted: 29 December 2020 ·
Published Online: 19 January 2021

Z. Yan,[1] J. J. Yun,[1] W. B. Sui,[1] L. Xi,[1] Z. T. Xie,[2,3] J. W. Cao,[1] M. S. Si,[1] D. Z. Yang,[1,a)] and D. S. Xue[1,a)]

AFFILIATIONS

[1]Key Laboratory for Magnetism and Magnetic Materials of Ministry of Education, Lanzhou University, Lanzhou 730000, China
[2]Department of Materials Science and Engineering, Guangdong Technion-Israel Institute of Science, Shantou, Guangdong 515063, China
[3]Technion—Israel Institute of Technology, Haifa 32000, Israel

Note: This paper is part of the Special Topic on Spin-Orbit Torque (SOT): Materials, Physics and Devices.
[a)]**Authors to whom correspondence should be addressed:** yangdzh@lzu.edu.cn and xueds@lzu.edu.cn

ABSTRACT

Recently, electrical switching of interface states in nonferromagnet/ferromagnet (FM)/antiferromagnet (AFM) heterostructure using spin–orbit torque (SOT) is promising due to its high efficiency, zero magnetic field, and multilevel memory state. However, the reversal mechanism of the AFM interface state is still unclear. In this work, we explained the bipolar current switching of the AFM interface state at zero magnetic field by spin–orbit torque (SOT) in a perpendicularly magnetized Pt/Co/IrMn multilayer. By considering symmetry, we reveal that the mechanism behind the AFM interface bipolar current switching is consistent with FM layers perpendicularly switching induced by SOT. The distinct AFM bipolar current switching by SOT is contributed to the symmetry broken by adjacent FM interface coupling. Under such broken symmetry, the antiparallel interface configuration (AP) between FM and AFM could be switched to parallel configuration (P) for both positive and negative currents; however, P is only allowed to be switched to the AFM multiple domain configuration (M), instead of AP. Our result will be helpful for the formulation of a comprehensive understanding of AFM switching induced by SOT and for the development of the interface AFM spintronic devices.

Antiferromagnet (AFM) has triggered renewed interest in the future information industry.[1,2] Compared to the ferromagnet (FM) order dominated information storage, such as magnetic tapes, hard disk, and magnetic random-access memory,[3,4] AFM order with a compensated magnetic moment can have its advantages for information storage and neuromorphic computing, such as magnetic field interference immunity, zero stray fields, high response frequency, multilevel memory state, and so on.[2,5–10]

Experiments and theories have demonstrated that AFM can be electrically efficiently manipulated by spin–orbit torque (SOT),[11–14] which can be divided into two categories. The first category is the manipulation of the bulk state of the AFM layer with in-plane magnetization.[9,10,13–20] Due to the local staggered effective field arising from SOT instead of the uniform magnetic field, the two spin sublattices of AFM can be rotated together, which makes it equally efficient as current-induced rotation in FM. The other category is the modulation of the AFM interface state in perpendicularly magnetized FM/AFM heterostructure.[21–23] For antiparallel configuration (AP) between FM and AFM at the interface, even at the zero magnetic field, the AFM interface magnetization can be switched to parallel configuration (P) for both positive and negative currents. However, unlike the previous SOT switching,[24–26] the AFM interface state cannot be electrically switched back from P to AP. Moreover, such AFM interface switching behavior in FM/AFM heterostructure does not require the auxiliary magnetic field and does not depend on the current polarity.[21] Therefore, it is still an open question to understand such AFM switching in the FM/AFM heterostructure.

In this work, we systemically study the AFM interface state switching under bipolar current in a perpendicularly magnetized FM/AFM heterostructure. First, we demonstrate that the switching of the AFM interface state can be understood by the broken symmetry due to the exchange coupling at the FM/AFM interface.[27] Second, we propose a reversible AFM interface switching process, where the AFM spin state can be freely switched back and forth between P and the AFM multiple domain configuration (M), by adjusting the current pulse and magnetic field. Finally, we demonstrate that M is high

tunability and stability when the amplitude of current pulse and magnetic field is changed, which will be useful for neuromorphic computing.

The film stack of Ta(2.6)/Pt(5.5)/Co(0.8)/$Ir_{20}Mn_{80}$(6.2)/Ta(1.3)/TaO_x(1.6) with perpendicular anisotropy (the numbers are layer thicknesses in nanometers) was deposited on the corning glass substrate by magnetron sputtering with a base pressure of 3.0×10^{-5} Pa. To electrically switch and detect the AFM interface state, the as-deposited film was patterned into 10 μm wide and 190 μm length Hall bar. The current pulse (the pulse period t = 10 μs in our work) was applied along the x-direction, and the SOT switching was detected by anomalous Hall measurement.

According to orientations, the SOTs are divided into two parts, named by Field-Like (FL) torque $\vec{\tau}_{FL} \propto \vec{m} \times \vec{\sigma}$ and Damping-Like (DL) torque $\vec{\tau}_{DL} \propto \vec{m} \times (\vec{\sigma} \times \vec{m})$, where $\vec{m}$ and $\vec{\sigma}$ are the unit vectors of the AFM sublattice magnetization and spin polarization, respectively.[24] When an in-plane current is applied through the Pt/Co/IrMn heterostructure in Fig. 1(a), the spin current J_s is generated by the Pt layer and its interface.[28,29] Because of the thin thickness of the Co layer (0.8 nm), the spin current can pass through the Co layer and exert SOTs on the interface magnetization of the IrMn layer.[30,31] For the perpendicularly magnetized IrMn, $\vec{\tau}_{FL}$ on the two AFM sublattices are antiparallel that cancels each other, while $\vec{\tau}_{DL}$ are even function of $\vec{m}$, indicating that $\vec{\tau}_{DL}$ on two AFM sublattices are parallel, thus providing a total torque to rotate the two AFM sublattice spins together in Fig. 1(a). However, under such SOTs in the perpendicularly magnetized AFM layer, switching from up to down is equal to switching from down to up. As a result, such switching cannot occur, which is forbidden due to the limitation of symmetry. To break the symmetry, an in-plane auxiliary magnetic field has to be used to provide additional torque,[32–35] which makes a favorite rotation direction. Unlike the above case that uses an external magnetic field to break the symmetry, the exchange coupling at the FM/AFM heterostructure interface naturally breaks the symmetry of the AFM interface.[36] The AFM interface magnetization favors the adjacent FM magnetization to minimize the interface coupling energy. As shown in Fig. 1(a), without the auxiliary magnetic field, the AFM interface state can be rotated clockwise and switched from AP to P. If the current is reversed, i.e., along the $-x$ direction, the AFM interface state switching still occurs, but the rotation direction is opposite to the positive current due to the inverse spin polarization. However, as shown in Fig. 1(b), such field-free AFM switching in FM/AFM cannot be switched back from P to AP again, which contrasts with the reported reversible electrical switching between the two orthogonal AFM bulk states by applying the current along with two orthogonal in-plane directions.[13,17]

Figure 1(c) shows the typical current-induced switching of the AFM interface state from AP to P in the Pt/Co/IrMn heterostructure. Owing to the AFM interface pinning effect,[27] the shift of the FM hysteresis loop by the amount of exchange bias field (H_E) is usually used to demonstrate the AFM interface state.[36] Similar to the

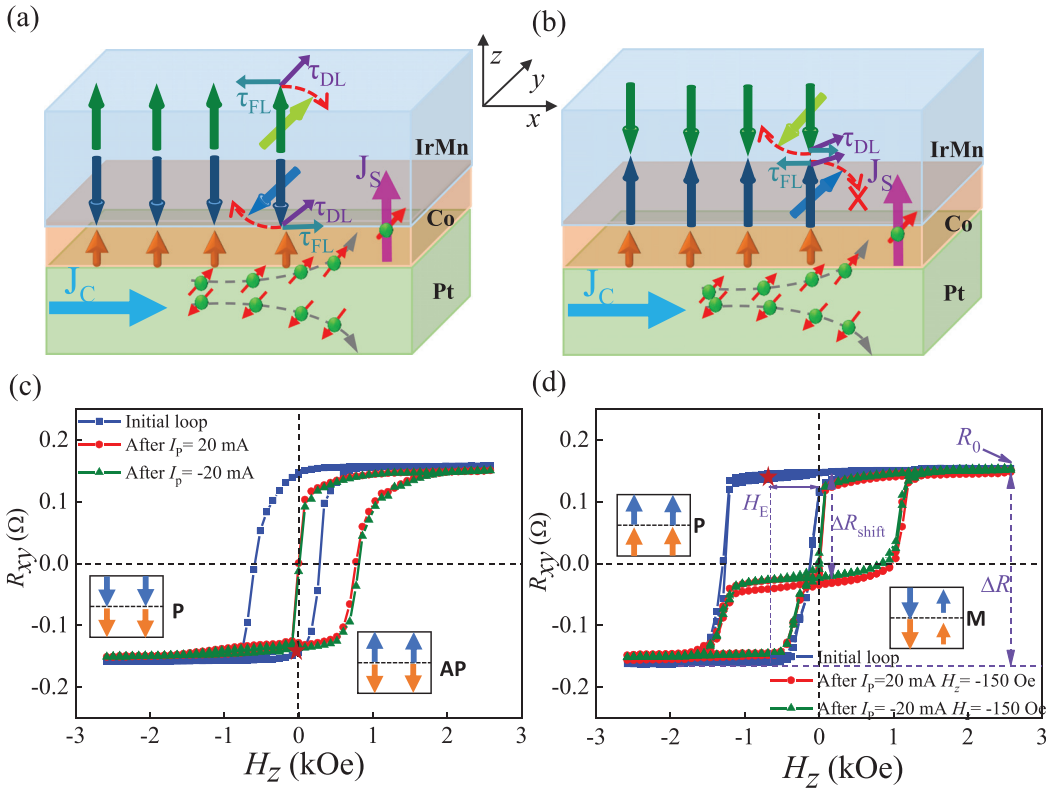

FIG. 1. (a) The schematic of the AFM interface state switching from AP to P is allowed in the Pt/Co/IrMn structure for a positive current pulse. (b) The switching from P to AP is forbidden. (c) The current-induced fully switching of the AFM interface state from AP to P. (d) The current-induced partially switching of the AFM interface state from P to M.

observations by Lin *et al.*,[21] after applying current pulse $I = \pm 20$ mA under zero magnetic field [the initial state marked as a star in Fig. 1(c)], H_E changes from negative to positive, representing the total switching of the AFM interface state from AP to P.

Figure 1(d) shows the typical current-induced switching of the AFM interface state from P to M in the Pt/Co/IrMn heterostructure. When applying a pulse current $I = \pm 20$ mA at a parallel interface state under a perpendicular magnetic field $H_z = 150$ Oe [the initial state marked as a star in Fig. 1(d)], a double-biased loop is observed in Fig. 1(d), representing the formation of M. Here, we define the multilevel remanence state (MRS) by the ratio of the height of shift-loop (ΔR_{shift}) to the total height of sub-loops (ΔR) at $H_z = 0$ Oe. MRS can be considered as the content of the partial switching of the AFM interface state. One can find that there is a little difference in MRS for the positive and negative current pulses in Fig. 1(d), which might result from the different switching energy under rotation clockwise and anticlockwise.

Figures 2(a) and 2(b) show the typical hysteresis loops after applying a different perpendicular magnetic field and current pulses. One can find that the MRS can be significantly controlled by both the magnetic field and current pulses. When current pulse $I_p = 20$ mA is fixed under different magnetic fields, MRS gradually increases with the increasing magnetic field, as shown in Fig. 2(a). Similarly, MRS also increases with the increasing amplitude of the current pulse under a fixed magnetic field $H_z = 150$ Oe, as shown in Fig. 2(b). Such AFM multiple domain states tuned by applying magnetic fields and current pulse have been reported in previous works,[22,23] which is attractive for neuromorphic computing and multiple state memories; however, the switching mechanisms to form M in these works are different. In our previous works,[22] we use current-induced SOT to switch FM by applying an in-plane auxiliary magnetic field. Owing to the partitional switching of FM, it rotates interface AFM spin together, thus M is formed. When the current pulse is large enough, MRS can reach one, indicating a complete switching. Here, we use the SOT to directly switch two AFM sublattice spins together. The formed M from P is ascribed to the competition between the current induced SOT and FM/AFM interface coupling. Again, one can also find that MRS cannot reach one due to symmetry limitations.

Unlike the irreversible AFM switching between P and AP at the FM/AFM interface, there is a reversible switching between P and M in Fig. 3. Figure 3(a) shows the MRS color map of AFM switching from P to M, where MRS = 0 is representing P, MRS = 1 is presenting AP, and other MRS value is representing M. It should be noted that the AFM switching from P to M only occurred under the negative magnetic field. Interestingly, the reversible switching back from M to P is observed in Fig. 3(b), where the switching can only occur under the positive magnetic field. We noted that the interface AFM spin switching is almost symmetric under the positive and negative current pulses for both Figs. 3(a) and 3(b). Moreover, the smaller amplitude of the current pulse requires a larger perpendicular magnetic field to switch the AFM spins, which is consistent with previous work,[23] and can rule out the conventional field-cooling effect due to current-induced Joule heating. Interestingly, we also noted that switching from M to P is

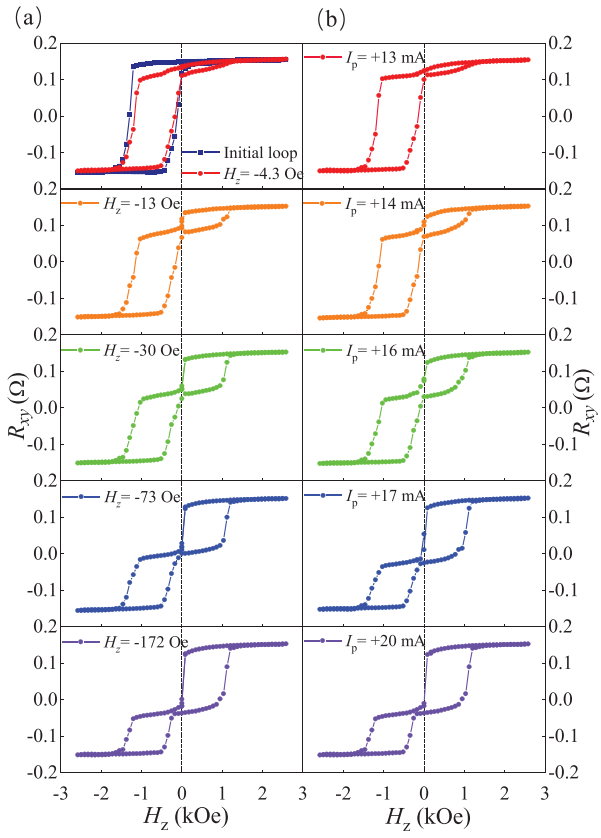

FIG. 2. The R_{xy}–H_z curves switched from P in the initial loop (a) after applying a current pulse $I_p = 20$ mA under different magnetic fields and (b) after applying a current pulse with different amplitudes under $H_z = 150$ Oe.

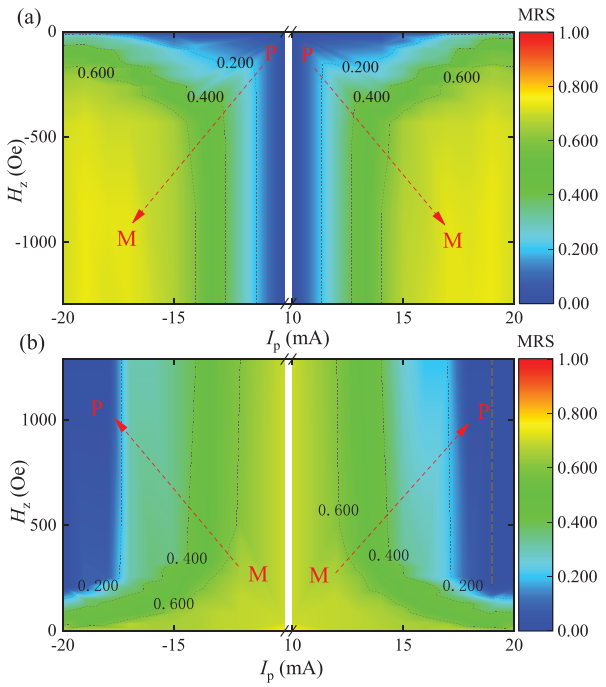

FIG. 3. The color map of MRS shows reversible switching (a) from P to M and (b) from M to P in the Pt/Co/IrMn heterostructure.

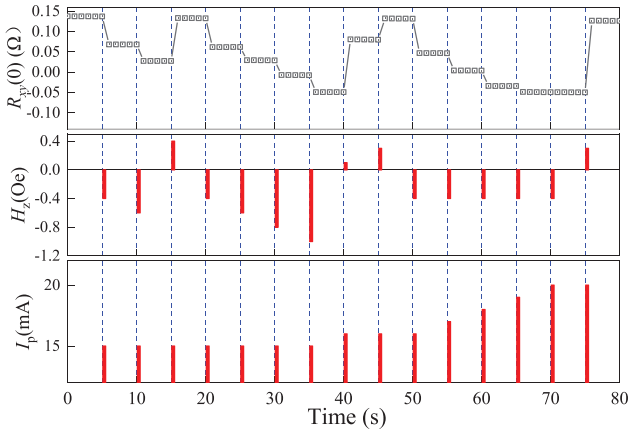

FIG. 4. Manipulating multilevel remanence state by applying various current pulses and magnetic fields.

easier than that from P state to M state. This is because the AFM/FM interface coupling can help AFM spin switching from M to P but hinder the switching from P to M.

Figure 4 show a high tunability and stability of M state at the AFM/FM interface by adjusting different currents and magnetic fields, which are attractive for neuromorphic computing, memristor, and logic operation basic devices.[9,10,37] In order to test whether M can be manipulated or not, the current pulses and magnetic fields with various amplitudes were applied. After applying a combination of current pulses and magnetic fields, R_{xy} at the zero magnetic field is recorded. One can easily find that the variation trend of R_{xy} significantly depends on the direction of the magnetic field. R_{xy} increases (decreases) for the positive (negative) magnetic field, no matter what the polarity of the current. Particularly, the evolution of M can be continuously manipulated by the current pulse and magnetic field, without being reset to the initial state. Moreover, the five recorded values of R_{xy} keep nearly constant after applying the current pulse and magnetic field, demonstrating a very high stability. It should also be noted that R_{xy} is immune to very strong magnetic fields even to several teslas, owing to the zero magnetization of AFM. These results demonstrate that the storage cell with relatively stable multilevel states tuned by SOT can be realized in Heavy Metal/FM/AFM multilayers.

In conclusion, we explain the physical mechanism of SOT switching AFM in Pt/Co/IrMn multilayers according to symmetry, where AFM can have two equivalent switching polarities under positive and negative currents. Although the AFM interface spin cannot be reversibly switched between P and AP, it can be manipulated back and forth between M and P, by applying a different perpendicular magnetic field and current pulse. This feature is attractive in the nonvolatile multilevel storage. We further demonstrate that the nonlinear evolution of M for Pt/Co/IrMn multilayers under various magnetic fields and current pulses has a high repeatability and stability, which is important for neuromorphic computing.

This work was supported by the NSFC of China (Grant Nos. 11774139, 11874189, 51372107, 51671098, 91963201, and 11674143), PCSIRT (Grant No. IRT-16R35), and the 111 Project under Grant No. B20063.

DATA AVAILABILITY

The data that support the findings of this study are available from the corresponding author upon reasonable request.

REFERENCES

[1]R. Duine, Nat. Mater. **10**, 344 (2011).
[2]M. B. Jungfleisch, W. Zhang, and A. Hoffmann, Phys. Lett. A **382**, 865 (2018).
[3]J. M. Daughton, J. Appl. Phys. **81**, 3758 (1997).
[4]C. Chappert, A. Fert, and F. N. Van Dau, Nat. Mater. **6**, 813 (2007).
[5]V. Baltz, A. Manchon, M. Tsoi, T. Moriyama, T. Ono, and Y. Tserkovnyak, Rev. Mod. Phys. **90**, 015005 (2018).
[6]T. Jungwirth, X. Marti, P. Wadley, and J. Wunderlich, Nat. Nanotechnol. **11**, 231 (2016).
[7]O. Gomonay, T. Jungwirth, and J. Sinova, Phys. Status Solidi RRL **11**, 1700022 (2017).
[8]J. Sinova and I. Žutić, Nat. Mater. **11**, 368 (2012).
[9]D. Kriegner, K. Výborný, K. Olejník, H. Reichlová, V. Novák, X. Marti, J. Gazquez, V. Saidl, P. Němec, V. V. Volobuev, G. Springholz, V. Holý, and T. Jungwirth, Nat. Commun. **7**, 11623 (2016).
[10]K. Olejník, V. Schuler, X. Marti, V. Novák, Z. Kašpar, P. Wadley, R. P. Campion, K. W. Edmonds, B. L. Gallagher, J. Garces, M. Baumgartner, P. Gambardella, and T. Jungwirth, Nat. Commun. **8**, 15434 (2017).
[11]J. Železný, H. Gao, K. Výborný, J. Zemen, J. Mašek, A. Manchon, J. Wunderlich, J. Sinova, and T. Jungwirth, Phys. Rev. Lett. **113**, 157201 (2014).
[12]J. Železný, H. Gao, A. Manchon, F. Freimuth, Y. Mokrousov, J. Zemen, J. Mašek, J. Sinova, and T. Jungwirth, Phys. Rev. B **95**, 014403 (2017).
[13]P. Wadley, B. Howells, J. Elezny, C. Andrews, V. Hills, R. P. Campion, V. Novak, K. Olejnik, F. Maccherozzi, S. S. Dhesi, S. Y. Martin, T. Wagner, J. Wunderlich, F. Freimuth, Y. Mokrousov, J. Kune, J. S. Chauhan, M. J. Grzybowski, A. W. Rushforth, K. W. Edmonds, B. L. Gallagher, and T. Jungwirth, Science **351**, 587 (2016).
[14]S. Yu. Bodnar, L. Šmejkal, I. Turek, T. Jungwirth, O. Gomonay, J. Sinova, A. A. Sapozhnik, H.-J. Elmers, M. Kläui, and M. Jourdan, Nat. Commun. **9**, 348 (2018).
[15]T. Moriyama, S. Takei, M. Nagata, Y. Yoshimura, N. Matsuzaki, T. Terashima, Y. Tserkovnyak, and T. Ono, Appl. Phys. Lett. **106**, 162406 (2015).
[16]L. Baldrati, C. Schmitt, O. Gomonay, R. Lebrun, R. Ramos, E. Saitoh, J. Sinova, and M. Kläui, Phys. Rev. Lett. **125**, 077201 (2020).
[17]M. Meinert, D. Graulich, and T. Matalla-Wagner, Phys. Rev. Appl. **9**, 064040 (2018).
[18]L. Baldrati, O. Gomonay, A. Ross, M. Filianina, R. Lebrun, R. Ramos, C. Leveille, F. Fuhrmann, T. R. Forrest, F. Maccherozzi, S. Valencia, F. Kronast, E. Saitoh, J. Sinova, and M. Kläui, Phys. Rev. Lett. **123**, 177201 (2019).
[19]C. Song, Y. You, X. Chen, X. Zhou, Y. Wang, and F. Pan, Nanotechnology **29**, 112001 (2018).
[20]S. Hu, H. Yang, M. Tang, H. Chen, Y. Yang, S. Zhou, and X. Qiu, Adv. Electron. Mater. **6**, 2000584 (2020).
[21]P. H. Lin, B. Y. Yang, M. H. Tsai, P. C. Chen, K. F. Huang, H. H. Lin, and C. H. Lai, Nat. Mater. **18**, 335 (2019).
[22]J. Yun, Q. Bai, Z. Yan, M. Chang, J. Mao, Y. Zuo, D. Yang, L. Xi, and D. Xue, Adv. Funct. Mater. **30**, 1909092 (2020).
[23]X. H. Liu, K. W. Edmonds, Z. P. Zhou, and K. Y. Wang, Phys. Rev. Appl. **13**, 014059 (2020).
[24]L. Liu, O. J. Lee, T. J. Gudmundsen, D. C. Ralph, and R. A. Buhrman, Phys. Rev. Lett. **109**, 096602 (2012).
[25]J. Kim, J. Sinha, M. Hayashi, M. Yamanouchi, S. Fukami, T. Suzuki, S. Mitani, and H. Ohno, Nat. Mater. **12**, 240 (2013).
[26]J. Nogués and I. K. Schuller, J. Magn. Magn. Mater. **192**, 203 (1999).
[27]L. Liu, C. F. Pai, Y. Li, H. W. Tseng, D. C. Ralph, and R. A. Buhrman, Science **336**, 555 (2012).
[28]J. Sinova, S. O. Valenzuela, J. Wunderlich, C. H. Back, and T. Jungwirth, Rev. Mod. Phys. **87**, 1213 (2015).
[29]I. Mihai Miron, G. Gaudin, S. Auffret, B. Rodmacq, A. Schuhl, S. Pizzini, J. Vogel, and P. Gambardella, Nat. Mater. **9**, 230 (2010).
[30]J. Bass and W. P. Pratt, J. Phys.: Condens. Matter **19**, 183201 (2007).

[31]K.-H. Ko and G.-M. Choi, J. Magn. Magn. Mater. **510**, 166945 (2020).
[32]S. Chen, D. Li, B. Cui, L. Xi, M. Si, D. Yang, and D. Xue, J. Phys. D **51**, 095001 (2018).
[33]M. Filianina, J.-P. Hanke, K. Lee, D.-S. Han, S. Jaiswal, A. Rajan, G. Jakob, Y. Mokrousov, and M. Kläui, Phys. Rev. Lett. **124**, 217701 (2020).
[34]W. Fan, J. Zhao, M. Tang, H. Chen, H. Yang, W. Lü, Z. Shi, and X. Qiu, Phys. Rev. Appl. **11**, 034018 (2019).
[35]X. Qiu, Z. Shi, W. Fan, S. Zhou, and H. Yang, Adv. Mater. **30**, 1705699 (2018).
[36]Y. Sheng, K. W. Edmonds, X. Ma, H. Zheng, and K. Wang, Adv. Electron. Mater. **4**, 1800224 (2018).
[37]X. Marti, I. Fina, C. Frontera, J. Liu, P. Wadley, Q. He, R. J. Paull, J. D. Clarkson, J. Kudrnovský, I. Turek, J. Kuneš, D. Yi, J.-H. Chu, C. T. Nelson, L. You, E. Arenholz, S. Salahuddin, J. Fontcuberta, T. Jungwirth, and R. Ramesh, Nat. Mater. **13**, 367 (2014).